URSI GASS 2021, Rome, Italy, 28 August - 4 September 2021

Personal Distributed Exposure Meters for the mm-Wave Band

R. Aminzadeh*(1), J. Sol(2), A. Thielens(1), P. Besnier(2), M. Zhadobov(2), L. Martens(1), and W. Joseph(2)
(1) Dept. of Information Technology, Ghent University/imec, B-9052 Ghent, Belgium
e-mail: reza.aminzadeh@ugent.be
(2) IETR, Institute of Electronics and Telecommunications of Rennes (IETR), UMR CNRS 6164
University of Rennes 1, 35042 Rennes, France
(*Invited Paper*)

Abstract

We investigated the possibility of using multiple antennas on the body to design personal distributed exposure meters for the mm-wave band. This was studied in terms of body shielding. Measurements were performed on a skin phantom in a mm-wave reverberation chamber and in a lab environment.

1 Introduction

The fifth generation of mobile networks (5G) will benefit from mm-waves to achieve high data rates [1]. Once this technology is on the market, it becomes crucial to measure personal exposure to electromagnetic fields (EMFs) in the mm-waves band. Personal exposure to radio-frequency EMFs is measured with personal exposure meters (PEMs). Research has shown that PEM's measurements are associated with large measurement uncertainties [2, 3, 4]. To reduce these uncertainties, a multi-band personal distributed exposure meter has been designed for the sub-6 GHz band [4, 5, 6]. Similarly, a distributed exposure meter was designed with three nodes on an arm of a subject [7]. The exposure meter of [7] has been extended to nine antennas [8]. However, none of the previously proposed mm-wave exposure meters [7, 8], deployed the antennas on different locations on the body. The high propagation loss and low penetration depth of mm-waves [9], raises this question of whether mm-wave personal exposure meters can benefit from distributed nodes all over the body or not? The goal of this paper is to demonstrate whether this is achievable or not.

2 Materials and Method

The goal of the measurements is to assess the possibility of measuring personal exposure to mm-waves (at 60 GHz) using personal distributed exposure meters with more than one antenna. A distributed exposure meter will consist of multiple antennas distributed over the body. In contrast to the sub-6 GHz frequencies, in the mm-wave band, the human body could shield the path between the wireless source (of exposure) and the receiver antenna(s) on the body. Therefore, the effect of body shielding on the received power on-body is studied.

2.1 Antenna

Two antennas were used in this study: A horn antenna (DRH67, RFspin, Czech Republic) was used as the transmitter (TX) and a wire with a length of 1 cm soldered to a V-band connector (see Fig. 1(a)) was used as the receiver (RX). The choice of wire as the antenna was to study the interaction of the antenna with the surface waves when the path between TX and RX is obstructed by a phantom emulating the human body.

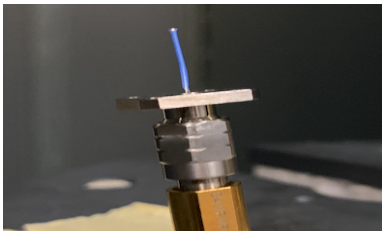

(a)

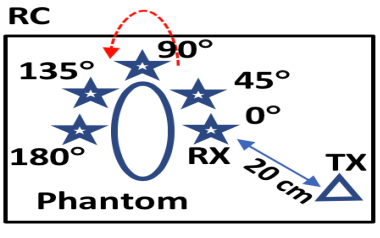

(b)

Figure 1. (a) A wire with length of 1 cm was used as the receiver antenna (RX) operating at 60 GHz. (b) The proposed measurement setup (top view) in the RC.

2.2 Skin phantom

A skin-equivalent phantom consisting of de-ionized water (500g), polyethylene powder (100g), Agar (7.5g), and TX-

151 (10g) [10] was fabricated in a spheroidal shape to mimick the human body with dielectric properties of human skin.

2.3 Reverberation Chamber

The mm-wave reverberation chamber (RC) is made of aluminum walls and is equipped with two vertical and horizontal stirrers. The dimension of the RC are $1.71\times1.46\times1.957\ m^3$.

2.4 Measurement Setup

The measurement setup is shown in Fig. 1(b). The measurements were performed in the mm-wave RC and were repeated in a lab environment. A ZVA-67 (Rohde and Schwarz, Germany) vector network analyzer (VNA) was used to feed the antennas and to measure the S-parameters. First, the quality factor of the RC was measured using the TX and RX for the loaded and unloaded RC [8]. For this, the RC was loaded with a container with similar dimensions to those of the skin phantom, filled with water. The goal of this measurement was to determine the sensitivity of the RC to the load (skin phantom), due to RC's large dimensions compared to the load (phantom).
Second, the RX was placed at 5 mm (1λ) from the phantom's surface to ensure the proper operation of the RX. The measurements were performed for 100 positions of the RC's stirrer in the 55-65 GHz range with steps of 10 MHz. The TX was placed at 20 cm from the RX and was fed with the VNA (0 dBm). Next, the RX was rotated from 0° to 180° around the phantom in steps of 45° and the measurements were repeated. The VNA measured the S-parameters for every position of the stirrer.
Third, the measurements of the previous step were repeated in a lab environment. In this case, the VNA measured the S-parameters for rotation of the RX between 0° and 180°.

3 Results

Figure 2 depicts the power reflection coefficient of the RX antenna on the front and back of the phantom. The RX has a reflection coefficient below -10 dB between 59 GHz and 62 GHz. Moving the RX from front to back of the phantom, decreases the power reflection coefficient by 5 dB which is due to the absorption of the mm-waves inside the phantom. In Figure 3, the Q-factor of the RC is illustrated for the loaded and unloaded RC. The Q-factor is between 4.1×10^4 and 7.1×10^4 for the unloaded RC. Although loading the RC decreases the Q-factor to a range of 3.8×10^4 to 5.9×10^4, these are sufficiently high values to ensure the correct functionality of the RC.

The transmission coefficients are shown in Figs. 4(a) and 4(b) for the measurements in the RC and in the lab environment, respectively. Clearly, the highest values in both cases are for 0° (-40 dB), where the RX is in front of the TX.

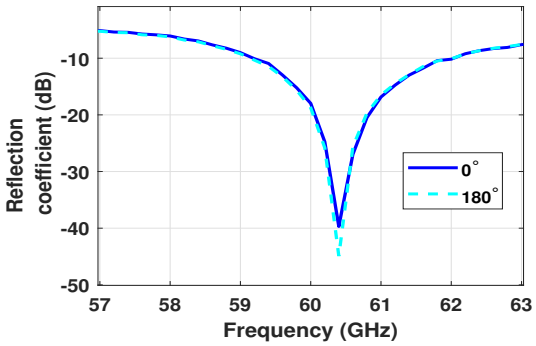

Figure 2. The on-phantom reflection coefficient of the RX for two locations on the phantom. 180° means that the path between the TX and RX is obstructed by the phantom.

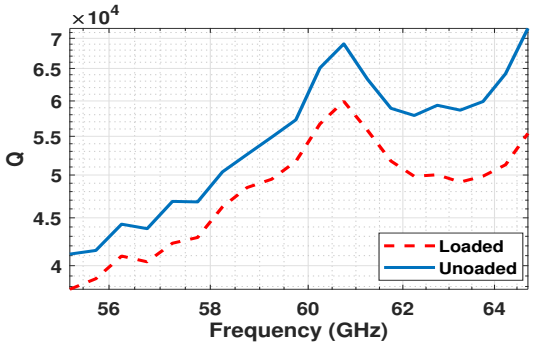

Figure 3. Quality factor of the RC for the loaded RC vs. unloaded.

For the RC's measurements at 60 GHz, rotating the RX decreases the transmission coefficient by 7 dB for every step of 45°. This means that the transmission coefficient reduces from -40 dB to -60 dB when the RX is rotated from 0° to 180°.
For the measurements in the lab, the difference between the transmission coefficient on the front and back of the phantom is about -28 dB and is up to -40 dB (at 59.4 GHz). This reduction (loss) is higher compared to the measurements in the RC. This is due to the fact that in the RC, the angles of incidence are uniform. This implies that in a diffuse environment (e.g., indoors) the opposite nodes of an exposure meter are less affected by the body shielding compared to specular fields. On-body path losses up to 52 dB has been reported in the literature for body parts such as neck, shoulder, and legs [11]. This is comparable to our findings that show a loss in the 28-40 dB range. It must be noted that the phantom used in this study is smaller than the body parts studied in [11].
Based on the results we suggest to first, using multiple antennas distributed on-body in a way that at least one antenna is always not shielded by the body; second, to perform on-body calibrations both in an RC and anechoic conditions; third, to deploy antenna arrays on the body with the possibility of using beam-steering for those arrays.

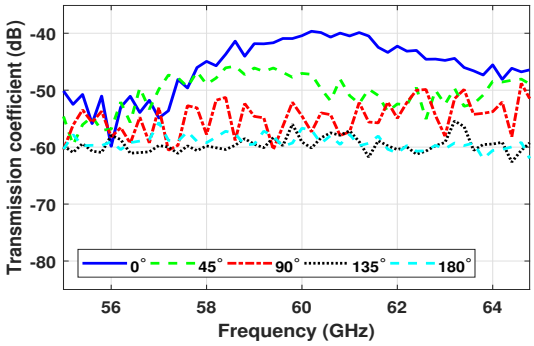

(a)

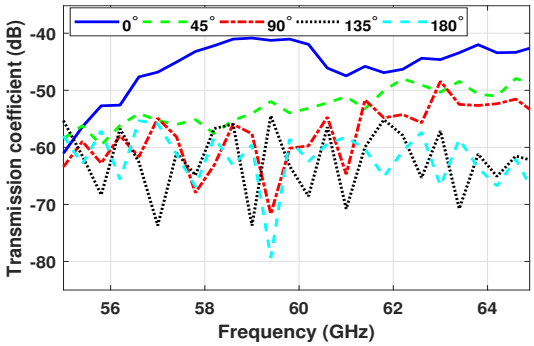

(b)

Figure 4. The transmission coefficient obtained from measurements in the RC (a) and a lab environment (b). For measurements in the RC (a), these values are averaged over 100 positions of the stirrer.

4 Conclusions

In this paper, we studied the effect of body shielding in the mm-wave band. The measurements indicate a loss in the range of 28-40 dB due to the body shielding for the measurements in a reverberation chamber and a lab environment. Based on the results, using multiple antennas on the body to design personal distributed exposure meters is achievable; however, smart deployment of antennas on the body is required.

5 Acknowledgements

R.A. received funding from FWO for part of this project via application nr. K233519N. A.T. has received funding from the European Union's Horizon 2020 research and innovation programme under the Marie Skłodowska-Curie grant agreement No 665501 with the FWO.

References

[1] A. Osseiran, F. Boccardi, V. Braun, K. Kusume, P. Marsch, M. Maternia, O. Queseth, M. Schellmann, H. Schotten, H. Taoka, H. Tullberg, M. A. Uusitalo, B. Timus, and M. Fallgren, "Scenarios for 5g mobile and wireless communications: the vision of the metis project," *IEEE Communications Magazine*, vol. 52, no. 5, pp. 26–35, May 2014.

[2] A. Thielens, S. Agneessens, L. Verloock, E. Tanghe, H. Rogier, L. Martens, and W. Joseph, "On-body calibration and processing for a combination of two radio-frequency personal exposimeters," *Radiation Protection Dosimetry*, vol. 163, no. 1, pp. 58–69, Jan. 2015.

[3] R. Aminzadeh, A. Thielens, A. Bamba, L. Kone, D. P. Gaillot, M. Lienard, L. Martens, and W. Joseph, "On-body calibration and measurements using personal radiofrequency exposimeters in indoor diffuse and specular environments: Calibration of Personal Exposimeters," *Bioelectromagnetics*, vol. 37, no. 5, pp. 298–309, Jul. 2016.

[4] R. Aminzadeh, A. Thielens, S. Agneessens, P. Van Torre, M. Van den Bossche, S. Dongus, M. Eeftens, A. Huss, R. Vermeulen, R. de Seze, P. Mazet, E. Cardis, H. Rogier, M. Röösli, L. Martens, and W. Joseph, "A Multi-Band Body-Worn Distributed Radio-Frequency Exposure Meter: Design, On-Body Calibration and Study of Body Morphology," *Sensors*, vol. 18, no. 1, p. 272, Jan. 2018.

[5] ——, "The effect of antenna polarization and body morphology on the measurement uncertainty of a wearable multi-band distributed exposure meter," *Annals of Telecommunications*, vol. 74, no. 1, pp. 67–77, Feb. 2019.

[6] R. Aminzadeh, A. Thielens, D. P. Gaillot, M. Lienard, L. Kone, S. Agneessens, P. Van Torre, M. Van den Bossche, L. Verloock, S. Dongus, M. Eeftens, A. Huss, R. Vermeulen, R. de Seze, E. Cardis, H. Rogier, M. Roosli, L. Martens, and W. Joseph, "A Multi-Band Body-Worn Distributed Exposure Meter for Personal Radio-Frequency Dosimetry in Diffuse Indoor Environments," *IEEE Sensors Journal*, vol. 19, no. 16, pp. 6927–6937, 2019.

[7] R. Aminzadeh, A. Thielens, H. Li, C. Leduc, M. Zhadobov, G. Torfs, J. Bauwelinck, L. Martens, and W. Joseph, "Personal Exposimeter for Radiation Assessment in Real Environments in the 60-GHz Band," *Radiation Protection Dosimetry*, vol. 176, no. 3, pp. 316–321, Nov. 2017.

[8] R. Aminzadeh, A. K. Fall, J. Sol, A. Thielens, P. Besnier, M. Zhadobov, N. De Geeter, P. P. Vasudevan, L. Dupré, R. Van Holen, L. Martens, and W. Joseph, "Design and Calibration of a mm-Wave Personal Exposure Meter for 5G Exposure Assessment in Indoor Diffuse Environments," *Journal of Infrared, Millimeter, and Terahertz Waves*, vol. 39, no. 12, pp. 1264–1282, Dec. 2018.

[9] T. S. Rappaport, S. Sun, R. Mayzus, H. Zhao, Y. Azar, K. Wang, G. N. Wong, J. K. Schulz, M. Samimi, and

F. Gutierrez, "Millimeter wave mobile communications for 5g cellular: It will work!" *IEEE Access*, vol. 1, pp. 335–349, 2013.

[10] N. Chahat, M. Zhadobov, S. Alekseev, and R. Sauleau, "Human skin-equivalent phantom for on-body antenna measurements in 60 ghz band," *Electronics Letters*, vol. 48, pp. 67–68(1), January 2012.

[11] C. Gustafson and F. Tufvesson, "Characterization of 60 GHz shadowing by human bodies and simple phantoms," in *2012 6th European Conference on Antennas and Propagation (EUCAP)*. Prague, Czech Republic: IEEE, Mar. 2012, pp. 473–477.